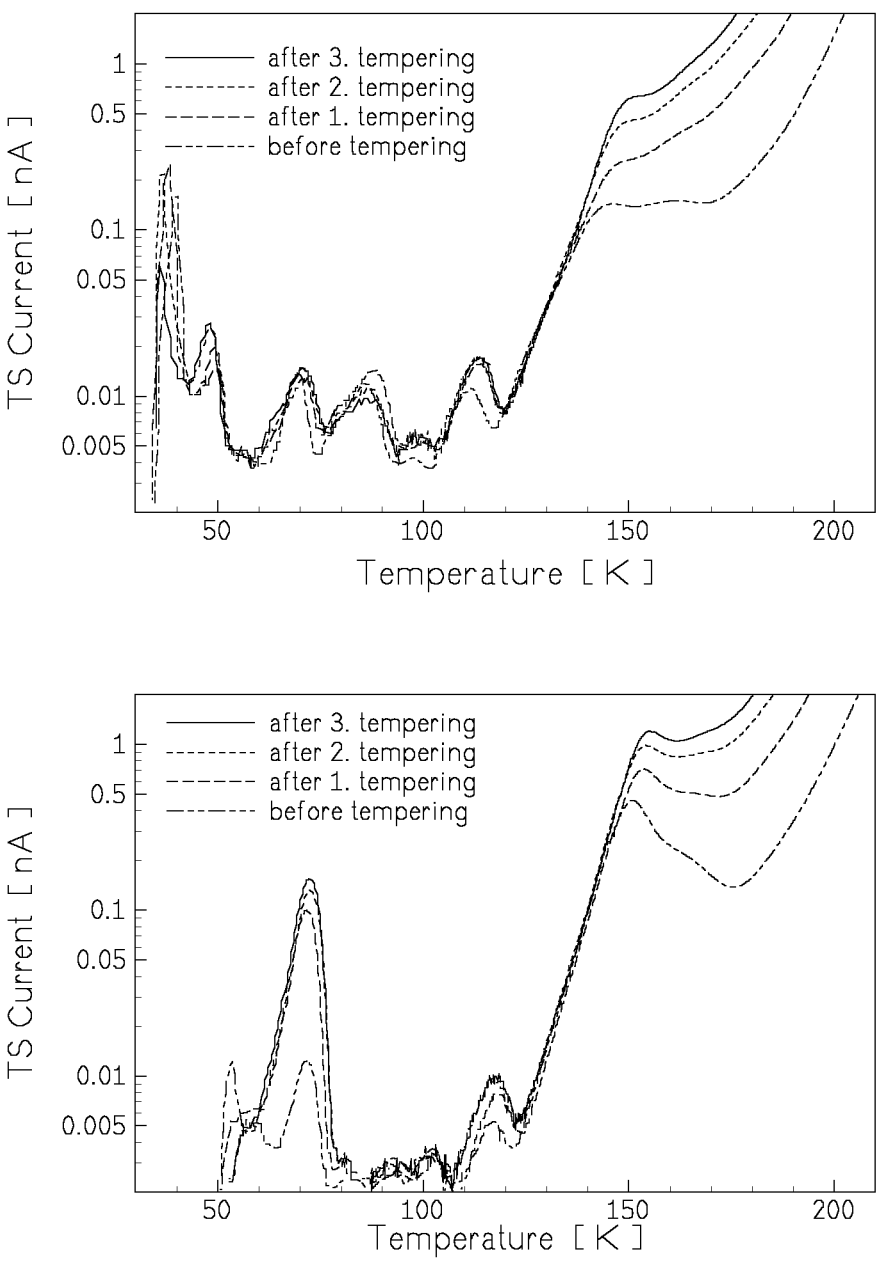

Figure 7.35: Change of TSC-spectrum due to heat treatments at 350 K. (a) Current injection at 35 K, (b) current injection at 50 K.

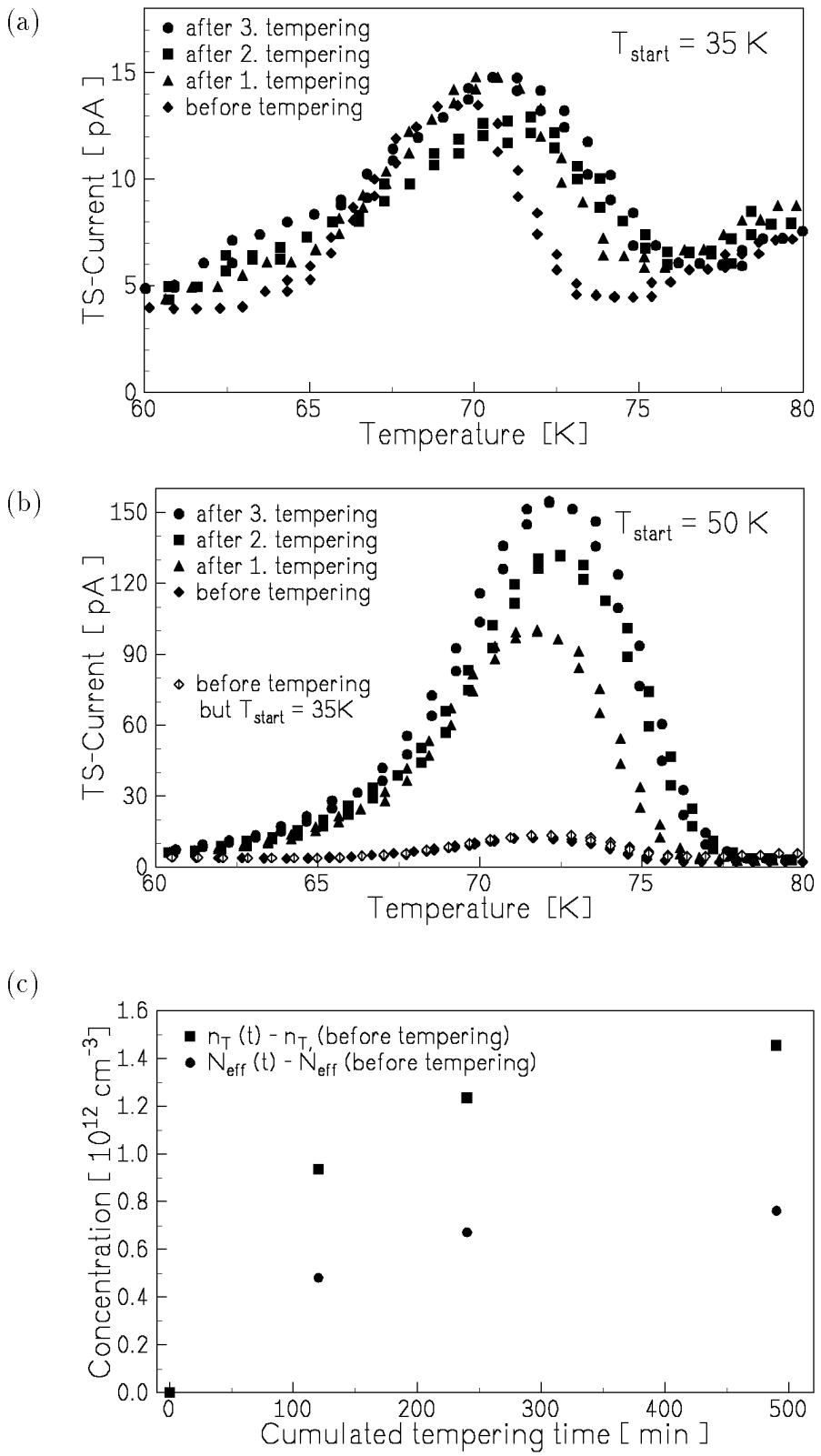

Figure 7.36: Bistable behaviour of peak E3. (a) No change of peak E3 due to the heat treatments can be seen if the level is filled at 35 K. (b) However, if the level is filled at 50 K an increase of peak E3 with tempering time can be observed. Note that before tempering the peak height did not depend on the start temperature. (c) Concentration of generated traps (assuming full depletion) and evolution of effective space charge during the heat treatment.

Tempering	Time $[min]$	V_{fd} $[V]$	N_{eff} [10^{11} cm^{-3}]	n_T [10^{11} cm^{-3}]	$\frac{n_T(t)-n_T(0)}{N_{eff}(t)-N_{eff}(0)}$
-	0	45	6.57	2.05	-
1	120	78	11.4	11.4	1.94
2	120	91	13.3	14.4	1.84
3	250	97	14.2	16.6	1.91

Table 7.11: Parameters and results of an isothermal heat treatment at 350 K. n_T has been determined according to eq. 4.65 (integration from t(60 K) to t(80 K), and N_{eff} from the depletion voltage eq. 2.26. Sample MUEA06, $\Phi = 2.14 \cdot 10^{13}$ cm^{-2}.

in n_T and N_{eff} (column far right). Note that the ratio has a constant value of about 2.

Before the heat treatment the height of peak E3 did not depend on the temperature of current injection (see fig. 7.36b). Hence it has to be concluded that a further defect is generated by the heat treatment, which has rather the same level parameters as the one existing already before the heat treatments and which exhibits a bistable behaviour. As described in sec. 3.3 the C_i-C_s complex has identical parameters to the A-centre and also arises during a heat treatment. Furthermore the C_i-C_s complex also provides the explanation for the bistable behaviour. Due to the configurational-coordinate energy diagram for the C_i-C_s pair the occurrence or absence of peak E3 can be explained the following way. Since during the cooling a reverse bias is applied the complex is not occupied by an electron and hence the state B of the defect is preferred energetically. However, during the current injection a certain fraction of pairs shifts from state B to state A. If the transition is assumed to be thermally activated from eq. 3.4 the time constant which controls the transition B $\rightarrow$ A can be calculated[10] : $\tau_{B\rightarrow A}(35K) = 2.5 \cdot 10^9$ s. Due to the short filling time (t_f=22 s), the number of switches from to B to A would be close to zero. And also at $T = 50$ K where the time constant is much smaller ($\tau_{B\rightarrow A}(50K) = 8.4 \cdot 10^2$ s) also less than 3 per cent of defects would undergo the transition from B to A. Thus thermal activation alone does not explain the transition of a considerable part of complexes. Hence, it has to be assumed that the current itself supplies the required energy for the transition at 50 K, while no transition is achieved at 35 K. Similar behaviour is known from the C_i-P_s pair (see sec. 3.3). The transition from one state to another by current injection is possible only at selected temperatures. A schematic of the model is shown in fig. 7.37. After the current injection during the delay ($\approx 2min$) the electrons bound at state B will be emitted very rapidly (ΔE_C= 0.11 eV) in contrast of those bound in state A (ΔE_C= 0.17 eV). Thus it is possible to detect the level by the occurrence of peak E3.

Because the C_i-C_s-complex is not charged in the SCR it is not possible to explain the reverse annealing directly by the generation of the carbon defect. However, the

[10] E=0.15 eV and $\hat{k}_0 = 6.4 \cdot 10^{-13}$ s^{-1} are taken from [11].

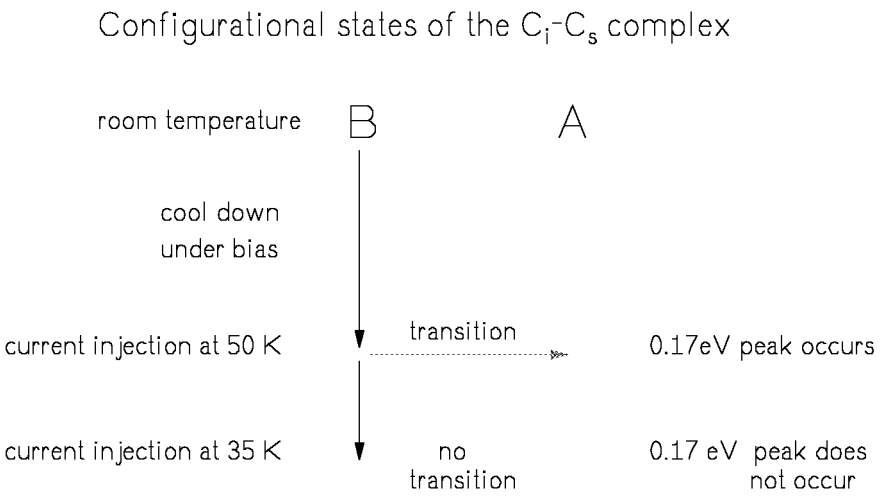

Figure 7.37: Schematic of a model for the bistable behaviour of peak E3 based on the C_i-C_s complex. At room temperature and under bias the configuration B is stable. Due to the current injection at 50 K a significant fraction of complexes undergoes transition B $\rightarrow$ A. Current injection at 35 K provides no or only insignificant transition.

constant ratio of the change in n_T to the change in N_{eff} (see tab. 7.11)

$$\frac{n_T(t) - n_T(0)}{N_{eff}(t) - N_{eff}(0)} \approx 2 \tag{7.12}$$

suggests that the increase of peak E3 and the reverse annealing are caused by the same phenomenon. Further investigation of this effect is necessary.

The 150 K peak increases also with tempering time, independent of the starting temperature. But it is not evident from the measurements whether or not this is caused by the steep increase of the current towards higher temperature.

7.3 Correlation of Detector Properties and Determined Defect Levels

In this section the effect of the determined defect properties on the effective doping concentration and the reverse current will be estimated. Furthermore the effect on the charge collection efficiency will be considered.

In order to get a survey of the contribution of the defects on the detector properties it is useful to calculate the room temperature emission rates. The values compiled in tab. 7.12 were obtained applying eqs. 2.42 and 2.43 and the defect parameters given in tab. 7.4. Comparing these values with the emission rates obtained in sec. 6.3 which are in the order of 10^4 s^{-1}, it becomes evident that the emission rates of E3, E4, E6a, and H1 are much higher. Only the emission rate of the E6b - level has the same order of magnitude as $e_{n,II}$ and $e_{n,\infty}$. Because in contrast to E6b which has been found to survive also an isochronal heat treatment up to 220°C,

Label	ΔE_T $[eV]$	$\sigma_{n,p}$ $[cm^2]$	$e_{n,p}$(RT) $[s^{-1}]$
E3	0.174	$1.13{\cdot}10^{-14}$	$3.5{\cdot}10^{9}$
E4	0.25	$5{\cdot}10^{-15}$	$7.6{\cdot}10^{7}$
E6a	0.39	$1.2{\cdot}10^{-15}$	$1.2{\cdot}10^{5}$
E6b	0.42	$1.0{\cdot}10^{-15}$	$3.6{\cdot}10^{4}$
H1	0.37	$5{\cdot}10^{-15}$	$3.4{\cdot}10^{5}$

Table 7.12: Emission rates at room temperature.

the component II of current and effective space charge anneals out already at room temperature, only the identification of $e_{n,E6b}$ with $e_{n,\infty}$ that was obtained from the non-annealing fraction of current and effective space charge is reasonable. Such an identification implies that N_C and J_∞ are caused by the 0.42 eV-level. Both quantities are of considerable relevance for the detector performance, hence further conclusions shall be plumbed here.

In a similar way as $\overline{\alpha_\infty}$ and b_C in sec. 6.3, now g_{E6b} and b_C are connected. N_T is given by $\Phi \cdot g_{E6b}$ and $\Phi \cdot b_C$ describes that part of N_C which grows in proportion to Φ. The offset $N_{C,0}$ must not be correlated with the current. From $N_C - N_{C,0} = N_T \cdot f_T$ (see eq. 6.27) follows :

$$f_T = \frac{N_C - N_{C,0}}{N_T} = \frac{\Phi b_C}{\Phi g_{E6b}} \approx 0.03. \tag{7.13}$$

Thus only a small fraction of the energy level is occupied by an electron and contributes to the space charge. Since also $f_T = e_p/(e_p + e_n)$ and e_n is known now the emission time constant for holes can be calculated by :

$$e_p = \frac{f_T e_n}{1 - f_T} \approx 1000 s^{-1}. \tag{7.14}$$

A complete determination of the defect-level parameters, namely ΔE_C and ΔE_V and the corresponding cross section σ_n and σ_p becomes possible now. $\Delta E_V = 0.70$ eV follows from $E_g - \Delta E_C$, and $\sigma_p = 7{\cdot}10^{-12}$ cm^2 can be obtained from eq. 2.43 with the result of eq. 7.14. From $e_p < e_n$ (equivalent to $f_T < 0.5$) follows that the generation process is governed by the hole emission, i.e. the emission of an electron from the valence band into the trap level is the bottle-neck of the current generation. Hence the temperature dependence of the bulk generation current should be governed by $\Delta E_V = 0.70$ eV.

This value is in good agreement with results obtained e.g. by Sotthibandu (0.6-0.8 eV) [119], Papendick (0.7 eV) [141] or Gill et al. (0.64 eV) [120]. However, also lower values in the range between 0.5 and 0.6 eV are cited in the literatue (e.g. [142]) and therefore a very careful study of the temperature dependence is desirable.

So far the supposed correlation of the 0.42 eV-level with the effective space charge and the reverse current is conclusive, but still suffers from the difference of the emission rates estimated from the DLTS-results and from the comparison of b_C and $\overline{\alpha_\infty}$ in sec. 6.3, which differ by a factor of about 2. The difference in

the low fluence range would be even greater if the exponential behaviour of $N_C(\Phi)$ would be taken into account. However, by none of the experimental findings it is proven that N_C represents only one type of defect. Thus a splitting into components C_i (i : 1 - n) is conceivable and the generation rate can be expressed as a sum : $b_C = b_{C,1} + b_{C,2} + \ldots + b_{C,n}$. The correlation of space charge, reverse current and the 0.42 eV -level becomes consistent (in the high fluence region) if only one of these components C_i contributes to the current, and if the corresponding generation rate is assumed to be $b_{C_i} = 7.6{\cdot}10^{-3}$ cm^{-1}. Then instead of the value obtained in eq. 7.15 the emission rate is found to be

$$e_{n,\infty} = \frac{\overline{\alpha_\infty}}{b_{C_i}\, q} \approx 36 \cdot 10^3 s^{-1}, \tag{7.15}$$

as required for consistency. Starting the calculation made above again from eq. 7.13 with b_{C_i} the values of f_T, e_p, and σ_p would drop about a factor of 2, but it still remains an open question whether the cross section for holes can be so large indeed.

None of the defect-levels E3, E4, E6a, E6b, or H1 is charged in the SCR under steady-state conditions, and thus they do not contribute to the effective space charge ($f_T \approx 0$).

The charge collection efficiency depends on the trapping time constant (see eq. 3.21), which is related to the fluence in the following way :

$$\frac{1}{\tau_T \Phi} = g_T v_{th} \sigma = \gamma_T. \tag{7.16}$$

In order to see how far the traps detected by DLTS contribute to the trapping the following estimate is made. The sum of all generation rates found for electron traps in high resistivity material is $g_{T,e}$= 1.64 cm^{-1}, and the cross section of all electron traps can be approximated by σ_n= 2·10^{-15} cm^2. The thermal velocity of electrons at room temperature is $v_{th,n}$= 1.12·10^7 cm s^{-1} and thus from eq. 7.16 follows :

$$\gamma_{T,e} \approx 4 \cdot 10^{-8} cm^2 s^{-1}. \tag{7.17}$$

The same way the trapping of holes can be estimated. It is g_{H1} = 1.2 cm^{-1} [11] and σ_{H1} = 2·10^{-15} cm^2. Hence with $v_{th,n}$= 1.56·10^5 cm s^{-1} it follows :

$$\gamma_{T,h} \approx 4 \cdot 10^{-8} cm^2 s^{-1}. \tag{7.18}$$

Both values are about a factor of 10 smaller than the results obtained by Fretwurst et al. [118], who found γ_T to be equal for electrons and holes in the fluence range $\Phi < 10^{13}$ cm^{-2} : $\gamma_{T,e,p}$ = 2.7·10^{-7} cm^{2}s^{-1}. The deviation will be even greater if the process of detrapping is taken into account. The charge collection measurements performed to obtain the trapping constants were usually made with a shaping time of 1 μs. Thus all charge carriers which are trapped in a shallow energy level (e.g. 0.17 eV) will be emitted immediately again and therefore not contribute to the charge loss. Only the emission time constant of the 0.42 eV-level (E6b, $\tau \approx 30$ μs) is significantly longer than the shaping time. Hence it has to be assumed that the trapping centres affecting the charge collection are even deeper than 0.42 eV and located close to the middle of the band gap.

[11] Trap H2 has been neglected here.

The trapping time constant of unirradiated material can be calculated by using the trap concentrations listed in tab. 7.2. For comparison with a value found experimentally in high resistivity material ($1/\tau_0 = 5.1{\cdot}10^4$ s^{-1}) by Wunstorf [36] the sum of trap concentrations ($6.2{\cdot}10^{10}$ cm^{-3}) found in the 941-material is used to obtain $1/\tau_0 = 1.4{\cdot}10^3$ s^{-1}. Also this value is too small to explain the experimental result.

Chapter 8

Summary and Conclusions

The long term behaviour of silicon detectors after neutron irradiation up to fluences $\Phi = 10^{14}$ cm^{-2} has been investigated at different temperatures. It has been found that the time dependence of the bulk generation current and the effective space charge can be described applying simple kinetic models as known from chemical reactions. The annealing of both quantities obeys first order processes. Two annealing stages were found for both current and space charge with rather similar room temperature time constants

$$\begin{aligned} \tau_I &\approx 2{\cdot}10^3 \text{ min}, \quad \text{and} \\ \tau_{II} &\approx 2{\cdot}10^4 \text{ min}. \end{aligned}$$

The similar time dependence of current and space charge suggests that both have the same origin, although the ratios of the corresponding amplitudes are different for current and effective space charge :

$$\frac{\alpha_I}{\alpha_{II}} = \frac{2.15 \cdot 10^{-17} A cm^{-1}}{1.84 \cdot 10^{-17} A cm^{-1}} \approx 1,$$
$$\frac{b_I}{b_{II}} = \frac{1.5 \cdot 10^{-2} cm^{-1}}{7.5 \cdot 10^{-3} cm^{-1}} \approx 2.$$

It is assumed that depending on the energy level parameters a certain fraction of the current generation centres is occupied constantly ($N_{SC} = N_T \cdot f_T$) and hence contributes to the effective space charge. While α is a measure of the total number of centres generated per fluence, the generation rate b reflects only the increase of the occupied centres. Thus the different ratios can be explained by assuming that the fractions of occupied levels are different for the components I and II.

Due to the long exposure times and the relatively low fluxes expected under operating condition, both annealing stages will be out of concern as long as the detector system is operated at room temperature. Already during the exposure most of the corresponding defects anneal out.

At lower temperature the situation is very different due to the retardation of annealing. Similar activation energies have been found for the annealing stages I and II of the current. Thus it is possible to describe the temperature dependence of the annealing using only the average value $E_a = 1.08$ eV. From eq. 6.25 follows that at $T = 0°$C the time constants for the current annealing are about 20 times longer, i.e. a month and 10 months respectively. Annealing processes in this time range are

considerable, because the defects cumulate. In case of current the problem is less urgent due to temperature reduction of the current.

Although a corresponding temperature dependence of the space charge annealing could not be confirmed by the measurements performed for this work, it is reasonable to assume significantly retarded annealing processes also for the space charge. In contrast to the current the accumulation of defects contributing to the effective space charge causes an increase of the depletion voltage (after type inversion) in any case which in turn requires a higher operational voltage.

In contrast to the current at room temperature which has been found to be stable in the long time range

$$\frac{\Delta J}{\Phi}(t \to \infty) = 4.4 \cdot 10^{-17} \text{ A cm}^{-1},$$

the effective space charge exhibits a pronounced reverse annealing. It has been shown that the reverse annealing can be modelled assuming the reaction of two electrically inactive defects to a complex which is charged in the SCR. Most probably the combining defects are of the same type, only for simplicity the parameters of the second order process were determined assuming two different types of defect of similar concentration. From experiments in the temperature range 5°C to 80°C the amplitude $N_{Y,\infty}$, the activation energy E_a and the frequency factor $\tilde{k}_0$ of the reverse annealing process were obtained :

$$N_{Y,\infty} = b_Y \Phi, \; b_Y = 0.053 \text{ cm}^{-1},$$

$$E_a = 1.29 \text{ eV, and}$$

$$\tilde{k}_0 = 294.7 \text{ cm}^3\text{s}^{-1}.$$

The generation rate b_Y agrees very well with values found by other authors who assumed a first order process. The activation energy is in a range which is reasonable for defect reaction and migration processes in silicon. In contrast the frequency factor is much higher (about 8 orders of magnitude) than expected from a correlation with the most abundant phonon frequency (10^{13} s^{-1}). A physical understanding of the high frequency factor has not been achieved so far.

Additionally to the acceptor-like states formed by the reverse annealing further electrically active defects are generated during the irradiation. The concentration of these defects remains constant in time. The fluence dependence can be described by

$$N_C(\Phi) = N_{C,0}(1 - \exp(-c_C \Phi)) + b_C \Phi,$$

where :

$$\begin{aligned} N_{C,0} &= 3.36 \; (\pm \; 0.03) \cdot 10^{11} \text{ cm}^{-3}, \\ c_C &= 3.58 \; (\pm \; 0.20) \cdot 10^{-13} \text{ cm}^2 \text{ and} \\ b_C &= 0.017 \pm 0.0001 \text{ cm}^{-1}. \end{aligned}$$

Because the fluence dependence of N_C can be separated into the exponential and the linear term, it is assumed that at least two different types of defects are contributing. $N_{C,0}$ is supposed to be correlated with the initial doping concentration. It is not evident from the experimental results how many different types of defects are summarised by the generation rate b_C.

From the annealing studies at lower temperature it is known that the reverse annealing at temperatures below 5°C is completely frozen. Since also the current can be reduced significantly by cooling (I(20°C)/I(0°C) = 0.15), it is inevitable to operate silicon detectors in high luminosity experiments such as the LHC at temperatures in the range between 0°C and 5°C.

The most prominent feature of the second order process is the half-life period which depends on the concentration of combining defects. The reverse annealing becomes faster with increasing concentration of the electrically inactive defect. This behaviour has a strong effect on the forecasting of operational scenarios (see e.g. [124]) which have to consider warm-up periods for service and maintenance to the detector system. Because during the long periods of operation at low temperature the inactive defects cumulate, the reverse annealing process will be very fast when the system is heated. This behaviour is significantly different from that expected for a first order process with a time constant independent of the concentration.

In general the operational voltage has to be increased in between the run-periods in order to maintain full depletion and high fields. Due to higher voltages also surface currents may occur additionally to the bulk generation current. Thus from the current damage constant and the generation rates of $N_{Y,\infty}$ and N_C only the lower limits of the operational parameters can be calculated.

The long term annealing has been parametrised using several fluence dependent quantities. Furthermore a fluence dependent effect has been found during the heat treatment, namely the decline of the effective space charge after tempering. The damage caused by neutrons of different energies can be normalised by applying the NIEL hypothesis. However, it is not obvious that the damage caused by other particles can be normalised the same way. Thus by comparing the different effects of damage induced by other particles, the NIEL hypothesis can be either confirmed or be called in question. The latter case could help to gain an insight into the detailed damage processes. From the comparison of damage caused by neutrons, protons and pions so far the NIEL hypothesis is not called in question [30, 143].

The investigation on defect characterisation has been performed applying the techniques of DLTS (deep level transient spectroscopy) and TSC (thermally stimulated current). The DLTS spectra were analysed utilising the Fourier-transformation of the measured transients. As opposed to the conventional analysis of maxima, the Fourier method is called direct analysis.

The DLTS investigation has been concentrated on electron traps. A typical spectrum recorded after irradiation showed up to seven peaks. Already before irradiation five peaks occur in spectra of oxide-passivated high resistivity material, only two peaks occur in the non-passivated material. No peaks were found in the spectra recorded with low resistivity material. The concentration of impurities is obviously too small in comparison to the effective doping concentration and hence below the detection limit. No or only little peaks can be seen in the spectra of the

p^+-n -samples.

An energy level

$$\Delta E_C = 0.53 \text{ eV and } \sigma_n = 3.5{\cdot}10^{-15} \text{ cm}^2,$$

has been found in both oxide-passivated and non-passivated material. These energy level parameters correspond very well with those of the gold acceptor. But the diffusion of gold into the bulk requires temperatures which are higher than those reached during the evaporation of gold or afterwards. If the gold was in the bulk already before the evaporation process, it should have been detected also in the p^+-n -samples which are fabricated from material of similar pureness.

Besides the 0.53 eV-level a second level at 0.15 eV is found in the spectra recorded on the non-passivated samples. A reasonable assignment for this level can not be proposed. The 0.15 eV-level does not occur in the spectra of the passivated samples. Perhaps it anneals out during the oxidation process.

In the oxide-passivated SB-samples four levels have been detected additionally to the 0.53 eV-level. The level at

$$\Delta E_C = 0.26 \text{ eV and } \sigma_n = 1.5{\cdot}10^{-17} \text{ cm}^2,$$

is known to be generated during high temperature step of the oxidation. Further levels $\Delta E_C = 0.24$ eV, $\Delta E_C = 0.12$ eV, and $\Delta E_C = 0.06$ eV could not be identified. But the 0.24 eV-level exhibits a metastable behaviour. It can be detected if the sample is cooled down without bias. Once the sample has been cooled under reverse bias voltage the peak does not appear in the spectrum and can not be recovered afterwards.

No levels could be detected in the p^+-n -samples. Only in one sample very small concentrations could be determined which are very close to the detection limit.

After irradiation three peaks occur in the spectra, independent of the material. The spectra are dominated by a peak in the temperature range 180 K - 210 K (peak E6). Two smaller peaks have maxima at 70 K - 90 K (peak E3) and at 100 K - 120 K (peak E4).

Applying a conventional analysis of maxima to the **peak E6** a single energy level can be determined. However, a direct analysis is not possible and also a recalculation of the measured peak according to the determined parameters fails. Hence the peak has been deconvoluted using two defect levels. The following level parameters allow the recalculation of the peak :

$\Delta E_C = 0.39$ eV and $\sigma_n = 1.2{\cdot}10^{-15}$ cm^2 (E6a), and
$\Delta E_C = 0.42$ eV and $\sigma_n = 1.0{\cdot}10^{-15}$ cm^2 (E6b).

These values have been confirmed by the results of an isochronal heat treatment (80°C - 220°C). Due to the heat treatment the peak decreased. The level parameters determined from the analysis of the remaining peak are similar to the parameters of E6b. Also the difference between the peaks before and after the heat treatment could be analysed, and the parameters were found to be similar to the parameters

of E6a.

The generation rates as determined from measurements performed 30 days after irradiation are :

$g_{E6a} = 0.34$ cm^{-1}, and
$g_{E6b} = 0.69$ cm^{-1}.

Both values are independent of the doping concentration of the material. With respect to the measurements performed 5 days after irradiation the concentrations of both levels decreased by a factor of about 0.79 (E6a) and 0.88 (E6b) respectively.

The 0.39 eV-level (E6a) is assigned to the single charged divacancy (V-V$^-$), because the parameters are in good agreement with values cited in the literature. However the annealing temperature of the V-V$^-$-complex is expected to be significantly higher than 220°C.

The 0.42 eV-level (E6b) could not be identified so far. Usually the 0.42 eV-level has been assigned to the E-centre (V-P). But the following experimental results contradict this assignment :

1.) The generation rate of the corresponding defect is independent of the initial phosphorus concentration, and

2.) the decrease of the peak due to an isochronal heat treatment is not correlated with a change of the effective doping concentration as expected in the case of the release of phosphorus.

Due to the high temperature which did not affect the 0.42 eV-level it could be concluded that, instead of the 0.39 eV-level which annealed during the tempering, the 0.42 eV-level should be assigned to the divacancy.

In the spectra measured from the non-passivated samples the **peak E4** is clearly dominated by an energy level

$\Delta E_C = 0.25$ eV and $\sigma_n = 5{\cdot}10^{-15}$ cm^2

which has been obtained from a direct analysis. In case of the oxide-passivated samples a direct analysis of the samples failed. Probably the energy level already observed prior to irradiation which has similar properties contributes significantly. Also the metastable behaviour occurs again. The above given level parameters allow the identification of the corresponding defect as the double charged divacancy (V-V$^=$), although the electron capture cross section is significantly greater than expected for a trap level which is negatively charged. The fluence dependence can not be described by a single generation rate, but the ratio n_T/Φ is higher in the case of material with a higher doping concentration and lower in the case of lower doped material. 30 days after irradiation the generation rate was found in the range

0.03 cm$^{-1} < g_{E4} < 0.16$ cm^{-1}.

However, this finding is supposed to reflect the dependence of the filling process on the doping concentration and not a doping dependent defect generation. The dependence on the doping concentration and thus on the free electron concentration is probably due to the very small capture cross section which is expected for the single

charged divacancy. The question remains as to why the value of σ_n as determined from the emission process is so big. The trap concentration increased by about 20% to 40% within the time between the 5th and the 30th day after irradiation.

The level parameters of the **peak E3** could be determined by a direct analysis independently of the material :

$\Delta E_C = 0.17$ eV and $\sigma_n = 1{\cdot}10^{-14}$ cm^2.

These values agree very well with the energy level parameters of the A-centre, but they also match the parameters of the C_i-C_s-complex. The generation rate determined 30 after irradiation is

$g_{E3} = 0.49$ cm^{-1}.

A 10% increase of the trap concentration has been observed with respect to measurements made 5 days after irradiation.

Two samples, a p-type SB-detector and a p^+-n -diode, were investigated also with respect to hole traps. The dominant hole trap occurs in the temperature range 180 K - 200 K. From the analysis of maxima an energy level (H1) :

$\Delta E_V = 0.36$ eV and $\sigma_n = 2{\cdot}10^{-15}$ cm^2

has been determined. These level parameters match those of the C_i-O_i-complex. The generation rate is $g_{H1} \approx 1.2$ cm^{-1}.

In contrast to the DLTS-technique which is limited to low defect concentrations the TSC-method can be used advantageous in the case of high defect concentrations. Thus it was possible to cover a fluence range up to 10^{14} cm^{-2}.

Prior to irradiation no spectra can be measured because the impurity concentration is below the detection limit. After irradiation the same energy levels which were determined by DLTS also dominate the TSC-spectrum, but a further peak occurs at fluences above 10^{12} cm^{-2}.

Three different methods of analysis were applied for comparison to the peak E3 and the results were found to agree exactly with the values determined by DLTS. But in case of the integral method, which has been introduced as a new method in this thesis, and the deconvolution method a temperature shift of 1.3 K has to be taken into account. The shift is due to an temperature gradient which originates from the rapid change in temperature. In contrast the method of delayed heating is based on the emission of charge carriers at a constant temperature, similar to DLTS.

The peak heights in the TSC-spectra depend on the measurement parameters. While the dependence on filling time and current is evident, the influence of the reverse bias voltage and the filling temperature differs from the expected behaviour. It has been found that the number of emitted charge carriers of the peak E3 grows in proportion to the square root of the voltage, even if the depletion voltage determined at room temperature is exceeded. Thus in contrast to the decrease of the depletion voltage with falling temperature as measured after low fluence irradiation,

in case of high fluences the depletion voltage at about 70 K is greater than at room temperature. The peak height of the peaks H1/E6 depends strongly on the filling temperature. The emitted charge increases with increasing filling temperature in the range between 35 K and 50 K by a factor of 3, above 50 K and below 35 K the peak height is constant. Also the peaks E3 and E4 were found to depend on the filling temperature. Hence for the comparison of concentration related results it is very important to have similar measurement conditions.

The fluence dependence of peak E3 can be separated into two regions. A steep increase occurs in the low fluence region, while above $\Phi = 1 \cdot 10^{12}$ cm^{-2} the increase is only moderate. The steep increase can be approximated by a generation rate which agrees with the value found from DLTS-measurements with p$^+$-n -samples : $g_{E3} = 0.8$ cm^{-1}. The generation rate which seems to be smaller at higher fluences is supposed to be a consequence of the temperature dependence of the depletion voltage. In the case of high fluences the assumption of full depletion at 70 K probably fails, but since the actual depletion depth is unknown the trap concentrations were calculated assuming full depletion in any case.

The fluence dependence of the peaks H1, E6a, and E6b was determined by applying the energy-level parameters as obtained from DLTS-measurements and fitting the trap concentrations. The following generation rates were found by averaging the n_T/Φ-ratio :

$g_{H1} = 0.37$ cm^{-1}, and
$g_{E6a} = 0.10$ cm^{-1}, and
$g_{E6b} = 0.12$ cm^{-1}.

As for the peak E3 in higher fluence range these values are significantly smaller than those obtained by DLTS indicating that the application of the room temperature depletion voltage is not sufficient to achieve full depletion also at lower temperature.

During an isothermal heat treatment at 350 K the peak E3 has been found to increase. However, the increase has been observed only if the filling temperature was 50 K. Measurements started after trap filling at 35 K do not show any change of peak E3 with tempering time. Hence, it is supposed that the increase is due to the formation of C_i-C_s-complexes which have energy level parameters similar to V-O-complex and also are known to exhibit a bistable behaviour. Although the C_i-C_s-complex is not responsible for the reverse annealing, strong indication for a close correlation is given by the fact that the increase of the trap concentration and the increase of the effective doping concentration due to the tempering time have a constant ratio of about 2.

A contribution of defect-levels E3, E4, E6a, and H1 to the effective space charge and to the reverse current of the detector can be excluded, because none of these levels is charged in the SCR, and the energy levels are too far from midgap for a significant generation rate. However, a certain fraction of the space charge and the total amount of the non-annealing current can be explained by the presence of the E6b-level with $\Delta E_C = 0.42$ eV and $\sigma_n = 1 \cdot 10^{-15}$ cm^2, if a hole capture cross section of about $4 \cdot 10^{-12}$ cm^2 is assumed. The concentration of E6b-levels as expected from the fluence dependence and the electron-hole pair generation rate as

determined by the energy level parameters explain completely the reverse current of the detector remaining after the short term annealing. The space charge originates from the fraction of the generation-levels which are constantly occupied. From the high annealing temperature of the 0.42 eV-level (T_{ann} >220°C) an identification as the single charged divacancy becomes suitable. The 0.42 eV-level contributes also to the charge trapping.

A defect-level which can be attributed to the reverse annealing has not been found. However, the reverse annealing was found to be correlated with the increase of a trap-level which is supposed to be the C_i-C_s-complex.

Hence the carbon-related defects and the 0.42-level have to be main subject of future studies on radiation hardness of silicon detectors.

Chapter 9

Appendix

Error in σ

From eq. 4.20 it follows that

$$\ln \frac{1}{\sigma} = -\frac{\Delta E_T}{k_B T} + \ln(\tau N_{C,V} v_{th,e,h}). \tag{9.1}$$

But instead of T a temperature $T + \Delta T$ has been measured, and instead of ΔE_T the energy $\Delta E'_T$ has been determined. Thus a wrong cross section will be determined :

$$\ln \frac{1}{\sigma'} = -\frac{\Delta E'_T}{k_B (T + \Delta T)} + \ln(\tau N_{C,V} v_{th,e,h}). \tag{9.2}$$

Using eq. 4.39 and applying the exponential function it follows :

$$\frac{1}{\sigma'} = \tau N_{C,V} v_{th,e,h} \exp\left(-\frac{\Delta E_T}{k_B T} \frac{(T + 2\Delta T)}{(T + \Delta T)}\right). \tag{9.3}$$

And thus the ratio of σ' and σ is given by :

$$\frac{\sigma'}{\sigma} = \frac{\exp\left(\frac{-\Delta E_T}{k_B T}\right)}{\exp\left(\frac{-\Delta E_T}{k_B T} \frac{T+2\Delta T}{T+\Delta T}\right)}. \tag{9.4}$$

With $\frac{T+2\Delta T}{T+\Delta T} \approx 1 + \frac{\Delta T}{T}$ it follows :

$$\frac{\sigma'}{\sigma} = \exp\left(\frac{\Delta E_T}{k_B T} \frac{\Delta T}{T}\right). \tag{9.5}$$

Exponential behaviour of C(t)

Eq. 4.49 in sec. 4.2.3 describes the capacitance as function of time taking into account that L_P and λ are not zero :

$$C(t) = \epsilon_S A \sqrt{\frac{(N_{eff} - n_T(t))}{\lambda^2 \frac{(n_{T,0} - n_T(t))^2}{(N_{eff} - n_T(t))} + 2V \frac{\epsilon_S}{q_o} - \lambda^2 (n_{T,0} - n_T(t)) - L_P^2 n_T(t)}}. \tag{9.6}$$

It is shown in the following, that the denominator is dominated by $2V\frac{\epsilon_S}{q_o}$:

$$2V\frac{\epsilon_S}{q_o} \gg \left|\lambda^2\left(\frac{(n_{T,0}-n_T(t))^2}{(N_{eff}-n_T(t))}-(n_{T,0}-n_T(t))\right)-L_P^2 n_T(t)\right|. \tag{9.7}$$

This can be done by comparing the estimated values of the single terms. First of all it is $2\frac{\epsilon_S}{q_o} = 1.3{\cdot}10^7$ (Vcm)$^{-1}$. Since most of the DLTS-measurements were performed with an applied voltage of 10 V or even a higher voltage, the left side of the relation in eq. 9.7 is $1.3{\cdot}10^8$ cm^{-1}. The value of λ depends on several parameters (see eq. 4.42). In order to apply the worst case it shall be assumed that $E_F - E_T = E_g/2$ and that the concentration of free electrons is as small as $n = 1{\cdot}10^{11}$ cm^{-1}. It follows that $\lambda < 8.6{\cdot}10^{-3}$ cm. Since it is always $n_{T,0} \geq n_{T,0} - n_T(t)$ and reasonable to assume $N_{eff} \gg n_T(t)$ as generally required for an exponential behaviour of the transient (see eq. 4.14) for the complete factor λ is multiplied with yields :

$$0 > \left(\frac{(n_{T,0}-n_T(t))^2}{(N_{eff}-n_T(t))}-(n_{T,0}-n_T(t))\right) > n_{T,0} \tag{9.8}$$

Assuming again a worse case it is $n_{T,0}$=$1{\cdot}10^{10}$ cm^{-3} and we get

$$\lambda^2\left|\left(\frac{(n_T(t)-n_{T,0})^2}{(N_{eff}-n_T(t))}-(n_{T,0}-n_T(t))\right)\right| < 7.4\cdot10^5\mathrm{cm}^{-1} \ll 1.3\cdot10^8\mathrm{cm}^{-1}. \tag{9.9}$$

The last figure to check is $L_P^2 n_T(t)$. As 10 V has been used mostly as reverse bias, the filling voltage used was almost 4 V. In order to find the corresponding value of L_P, it is firstly needed to determine W(4V) and then to subtract λ ($L_P = W - \lambda$). According to eq. 2.24 W(V) is proportional to the inverse square root of the effective doping concentration. Therefore again for a worst case assumption, N_{eff} is chosen to be as small as $1{\cdot}10^{11}$ cm^{-3}. In connection with the corresponding value of λ calculated above, we get

$$L_P(4V) = W(4\mathrm{V}) \text{ - } \lambda = 230\mu m \text{ - } 86\mu m = 144\mu m$$

and thus

$$L_P^2 n_T(t) = 2.07{\cdot}10^6 \text{ cm}^{-1},$$

if $n_T(t) = 1{\cdot}10^{10}$ cm^{-3} as assumed already above.

Finally it can be stated that indeed

$$2V\frac{\epsilon_S}{q_o} \gg 7.4\cdot10^5\mathrm{cm}^{-1} + 2.1\cdot10^6\mathrm{cm}^{-1}. \tag{9.10}$$

However, in order to be on the safe side the high resistivity material has been measured with a reverse bias of 20 V. It has to be emphasised that in case of low resistivity material the voltage related term is even more dominant, because λ decreases with increasing n_0.

Derivation of ΔC

According to eq. 4.50 it is

$$C_0 = \epsilon_S A \sqrt{\frac{(N_{eff} - n_{T,0})}{2V\frac{\epsilon_S}{q_o} - L_P^2 n_{T,0}}}. \tag{9.11}$$

Due to eq. 2.24 we can substitute $2V\frac{\epsilon_S}{q_o}$ with $W^2 N_{eff}$ and then write :

$$C_0 = \epsilon_S A \sqrt{\frac{(N_{eff} - n_{T,0})}{W^2 N_{eff}(1 - \frac{L_P^2}{W^2}\frac{n_{T,0}}{N_{eff}})}}, \tag{9.12}$$

or :

$$C_0 = \frac{\epsilon_S A}{W}\sqrt{\frac{(N_{eff} - n_{T,0})}{N_{eff}}}\frac{1}{\sqrt{1 - \frac{L_P^2}{W^2}\frac{n_{T,0}}{N_{eff}}}}. \tag{9.13}$$

Approximating $\sqrt{\frac{(N_{eff}-n_{T,0})}{N_{eff}}}$ by $1 - n_{T,0}/2N_{eff}$ (due to $N_{eff} \gg n_{T,0}$)

and $\frac{1}{\sqrt{1-\frac{L_P^2}{W^2}\frac{n_{T,0}}{N_{eff}}}}$ by $1 + (L_P^2/W^2)(n_{T,0}/2N_{eff})$ it follows :

$$C_0 = \frac{\epsilon_S A}{W}\left(1 - \frac{n_{T,0}}{2N_{eff}}\right)\left(1 + \frac{n_{T,0}L_P^2}{2N_{eff}W^2}\right). \tag{9.14}$$

In a similar way it follows from eq. 4.51 that :

$$C_E = \frac{\epsilon_S A}{W}\frac{1}{\sqrt{1 + \frac{\lambda^2 n_{T,0}}{W^2 N_{eff}}(\frac{n_{T,0}}{N_{eff}} - 1)}} \approx$$
$$\frac{\epsilon_S A}{W}\left(1 + \frac{\lambda^2}{W^2}\frac{n_{T,0}}{2N_{eff}}(1 - \frac{n_{T,0}}{N_{eff}})\right). \tag{9.15}$$

Since the approximation of the square root took only first order expression $\frac{n_{T,0}}{2N_{eff}}$, expressions of higher order will be neglected consistently in the following. Thus the difference $C_E - C_0 = \Delta C$ is given by :

$$\Delta C \approx \frac{\epsilon_S A}{W}\left(1 + \frac{n_{T,0}\lambda^2}{2N_{eff}W^2} - 1 - \frac{n_{T,0}L_P^2}{2N_{eff}W^2} + \frac{n_{T,0}}{2N_{eff}}\right) =$$
$$\frac{\epsilon_S A}{W}\frac{n_{T,0}}{2N_{eff}}\left(\frac{W^2 + \lambda^2 - L_P^2}{W^2}\right). \tag{9.16}$$

This expression differs slightly from that cited in [85]

$$\Delta C \propto \frac{L_R^2 - L_P^2}{W^2} = \frac{(W - \lambda)^2 - L_P^2}{W^2}. \tag{9.17}$$

List of Figures

2.1 Energy diagram for n- and p-type silicon 6
2.2 Impurity concentration in float-zone silicon 7
2.3 Abrupt p-n junction 8
2.4 Potential barrier at the Schottky contact 9
2.5 Emission and capture processes 13
2.6 Occupation probability in the SCR 16
2.7 Charge state of donors and acceptors 16
2.8 Schematic plot of detector operation 17
2.9 Fabrication process 19
2.10 Section of inner detector 21
2.11 Expected equivalent fluence per year in the SCT 21

3.1 NIEL and displacement damage cross-section versus neutron/particle energy 25
3.2 Various possible defect configurations 26
3.3 Local disturbance of the band structure caused by a cluster 27
3.4 Energy levels of vacancy related defects 31
3.5 Configurational co-ordinate energy diagram for the C_i-C_s complex . . 33
3.6 Effects of defects 35

4.1 Equivalent circuit of a reverse-biased diode 38
4.2 Frequency and temperature dependence of CV-measurements after irradiation 38
4.3 Determination of V_{fd} 40
4.4 Comparison of different methods of N_{eff}-determination 40
4.5 Current versus-square root of voltage 42
4.6 DLTS pulse sequence 44
4.7 Formation of a DLTS-peak 45
4.8 Correlator functions used for analysis of maxima 47
4.9 Analysis of maxima and corresponding Arrhenius-plot 48
4.10 Direct analysis and corresponding Arrhenius-plot 50
4.11 Charge distribution after the filling pulse 53
4.12 TS-Current as function of temperature 57
4.13 TS-Current as function of time 57
4.14 Method of delayed heating 59
4.15 The deconvolution method 60
4.16 TSC-peak divided into two parts at time t_x 61
4.17 Arrhenius plot from integral analysis 61

4.18 Variation of the heating rate 62

5.1 Schematic plot of test structures 65
5.2 Flux as function of distance 67
5.3 Schematic of circuit diagram 69
5.4 DLTS set-up 70
5.5 The cooling system with Peltier device 71
5.6 The helium and nitrogen cryostats 72

6.1 Effective doping concentration as function of fluence 76
6.2 Depletion voltage and ΔN_{eff} as function of time 77
6.3 Comparison of 1 and 2 order assumption 79
6.4 Comparison of half-life period 79
6.5 Development of ΔN_{eff} before and during heat treatment 80
6.6 Defect concentration of reverse annealing N_Y versus fluence 82
6.7 Introduction rate b_Y of various detector types 82
6.8 Concentration of constant defects versus fluence 83
6.9 Comparison of fluence dependence of ΔN_{eff} and N_C 84
6.10 $N_{C,0}$ versus $N_{eff,0}$ 84
6.11 Arrhenius plot of second order reaction constant 85
6.12 Fluence dependence of the reaction constant 86
6.13 Reverse annealing at lower temperature 87
6.14 Isochronal heat treatment 88
6.15 Comparison of Arrhenius plots of first and second order reaction constant 88
6.16 Comparison of half-life periods calculated from two different assumptions 91
6.17 Decline of depletion voltage after heat treatment 92
6.18 Depletion voltage versus cumulated tempering time 93
6.19 Schematic of the bistable defect 93
6.20 Concentration of the bistable defect normalised to fluence 94
6.21 Short term annealing of n- and p-type samples irradiated with high fluences 95
6.22 Short term annealing at lower temperatures 96
6.23 CV-measurements at different temperatures 98
6.24 Frequency dependence of depletion voltage at various temperatures . 99
6.25 Change of effective space charge versus temperature 99
6.26 Effective space charge versus fluence 100
6.27 Fluence dependence and annealing behaviour of reverse current . . . 102
6.28 Fluence dependence of reverse current 103
6.29 Time dependence of reverse current 104
6.30 Fitted time dependence of reverse current 104
6.31 Current annealing during heat treatments 105
6.32 Comparison of current annealing in p- and n-type material 106
6.33 Annealing of reverse current at lower temperature 108
6.34 Time constants of different annealing stages versus inverse temperature 110
6.35 Demonstration of the scaling factor 111

7.1 Characteristic spectrum after irradiation of a n-type sample 115
7.2 Concentration of occupied traps as function of filling time 117
7.3 Spectra before irradiation 119
7.4 Multistable defect level in DLT-spectrum before irradiation 120
7.5 DLT-spectrum of a p^+-n -sample before irradiation 121
7.6 Characteristic spectrum after irradiation of n-type sample 123
7.8 Recalculation of the peak E4 124
7.7 Deconvolution of peak E6 125
7.9 Multistable behaviour of peak E4 126
7.10 Parameters of peak E3 127
7.11 Spectra after irradiation of various fluences 129
7.12 Correlation between DLT-spectra and temperature dependence of N_{eff} 130
7.13 Fluence dependence of trap concentration 131
7.14 Time dependence of peak height 134
7.15 Isochronal heat treatment of a p^+-n -sample 136
7.16 Characteristic spectrum after irradiation of p-type sample 138
7.17 Typical TSC-spectrum 139
7.18 Assignment of peaks in the TSC-spectrum 140
7.19 Determination of energy level parameters by the delayed heating method 142
7.20 Determination of energy level parameters by the integral method and the deconvolution method 144
7.21 TSC-spectra for different filling times 145
7.22 TSC-spectra for different filling currents 145
7.23 Emitted charge versus injected charge 146
7.24 Forward current characteristics with temperature as parameter 147
7.25 TSC-spectra recorded after different filling voltages 147
7.26 TSC-spectra for different bias voltages 148
7.27 Emitted charge versus square root of reverse bias 149
7.28 TSC-spectra with filling temperature as parameter 150
7.29 Peak maximum as function of start temperature 150
7.30 TSC-spectra for various fluences 151
7.31 Fluence dependence of trap concentration corresponding to peak E3 . 152
7.32 Effective space charge at 70 K vs. fluence 154
7.33 Double peak simulated applying results from DLTS for various fluences 155
7.34 TSC-spectra of SB-samples 156
7.35 Change of TSC-spectrum due to heat treatments 157
7.36 Bistable behaviour of peak E3 158
7.37 Schematic of a model for the bistable behaviour of peak E3 160

List of Tables

3.1 Survey of possible defect reactions 26
3.2 Temperature and conditions for configuration transitions of the C_i-P_s complex 32
3.3 Energy levels of carbon related defects 33

5.1 Detectors used for the investigation 66
5.2 Survey of irradiation facilities 67

6.1 Parameters for donor removal and acceptor creation 76
6.2 Annealing parameters of the effective doping concentration 77
6.3 Parameters of reverse annealing at low temperature 89
6.4 Results of isochronal heat treatments 89
6.5 Summary of second order model 90
6.6 Individual results of investigation on the bistable defect 95
6.7 Damage constant α from different experimenters 101
6.8 Annealing parameters of the reverse current 101
6.9 Parameters of samples for current annealing at low temperature . . . 107
6.10 Individual annealing parameters 109
6.11 Comparison of annealing parameters of the effective doping concentration and the reverse current 112

7.1 Material used for the DLTS investigation 117
7.2 Energy levels in non-irradiated material 119
7.3 Energy levels in non-irradiated MPI-samples 122
7.4 Properties of radiation induced peaks 127
7.5 Generation rates 132
7.6 Generation rates of E6a and E6b 132
7.7 Annealing of trap concentrations 135
7.8 Parameters of hole traps 137
7.9 Recalculation of a TSC-spectrum using parameters obtained from a DLTS-measurement 141
7.10 Results of different methods of peak analysis 143
7.11 Parameters and results of an isothermal heat treatment 159
7.12 Emission rates at room temperature 161

Bibliography

[1] G. Hall. Semiconductor particle tracking detectors. *Rep. Prog. Phys.*, 57:481–531, 1994.

[2] E. Borchi and M. Bruzzi. *Radiation Damage in Silicon detectors.* La Rivista del Nuovo Cimento, Vol. 17, No. 11. Editrice Compositore, Bologna, 1994.

[3] H.G. Grimmeis and C. Ovren. Fundamentals of junction measurements in the study of deep energy levels in semiconductors. *J. Phys. E: Sci. Instrum.*, 14:1032, 1981.

[4] J. Bourgoin and M. Lannoo. *Point defects in semiconductors II, Experimental aspects.* Solid State Sciences 35. Springer-Verlag, Berlin, 1983.

[5] E. Spenke. *Elektronische Halbleiter.* Springer Verlag, Berlin, Heidelberg, New York, 1965.

[6] S.M. Sze. *Physics of Semiconductor Devices.* John Wiley & Sons, New York, Chichester, Brisbane, Toronto, Singapore, second edition, 1981.

[7] A. van der Ziel. *Solid State Electronics.* Prentice-Hall,Inc, London, 1968.

[8] W. v. Ammon and H. Herzer. The production and availability of high resistivity silicon for detector application. *Nucl. Instr. & Meth. in Physics Research*, A226:94, 1984.

[9] P. Dreier. High resistivity silicon for detector applications. *Nucl. Instr. & Meth. in Physics Research*, A288:272, 1990.

[10] G. Davies, E.C. Lightowlers, R.C. Newman and A.S. Oates. A model for radiation damage effects in carbon-doped crystaline silicon. *Semicond. Sci. Technol.*, 2:524, 1987.

[11] L.W. Song, X.D. Zhan, B.W.Benson and G.D.Watkins. Bistable interstitial carbon - substitutional-carbon pair in silicon. *Physical Review*, B42(9):5765, 1990.

[12] P. Siffert and A. Coche. New results on the rectifying process in surface barrier counters. *IEEE Transactions on Nuclear Science*, NS12(1):284, 1965.

[13] S.M. Sze. *Semiconductor Devices, Physics and Technology.* John Wiley & Sons, New York, Chichester, Brisbane, Toronto, Singapore, 1985.

[14] R. Wunstorf. Untersuchungen zur Diodencharakteristik von Silizium-Oberflächensperrschichtdetektoren. Staatsexamensarbeit, Universität Hamburg, September 1986.

[15] R.H. Richter. private communication.

[16] E. Fretwurst et al. Silicon detector developments for calorimetry : technology and radiation damage. *Nucl. Instr. & Meth. in Physics Research*, A288:1, 1990.

[17] E. Fretwurst, R. Grube, G. Lindström and J. Nagel. Development of large area Si-detectors —special properties and radiation stability—. *Nucl. Instr. & Meth. in Physics Research*, A253:467, 1987.

[18] W. Shockley and W. T. Read. Statistics of the recombination of holes and electrones. *Physical Review*, 87(5):835, 1952.

[19] E.H. Rhoderick and R.H. Williams. *Metal-semiconductor contacts.* Monographs in Electrical and Electronic Engineering. Clarendon Press, Oxford, second edition, 1988.

[20] G.F. Knoll. *Radiation detection and measurement.* John Wiley & Sons, New York, Chichester, Brisbane, Toronto, 1979.

[21] G. Hall. *Silicon detector and signal processing experiment.* Document for Second ICFA School on instrumentation in elementary Particle physics, find a better source, 1989.

[22] J. Kemmer. Fabrication of low noise silicon radiation detectors by the planar process. *Nucl. Instr. & Meth. in Physics Research*, A169:499, 1980.

[23] J. Kemmer. Improvement of detector fabrication by the planar process. *Nucl. Instr. & Meth. in Physics Research*, A226:86, 1984.

[24] P. Schlichthärle. Untersuchungen an Oberflächeneffekten in Silizium-Detektoren nach Schädigung mit 20 keV Elektronen. Diploma thesis, Universität Hamburg, 1995.

[25] W. Hildesheim and M. Seidel. An investigation into the radiation damage of the silicon detectors of the H1 plug calorimeter within the HERA environment. DESY Report 95-139, July 1995, submitted to Nuclear Instruments and Methods, 1995.

[26] ATLAS technical proposal for a general-purpose pp experiment at the Large Hadron Collider at CERN. CERN/LHCC/94-43, December 1994.

[27] Technical proposal backup document for the SemiConductor tracker SCT for the ATLAS Detector at the Large Hadron Collider at CERN. Working Document - Version 1.0.

[28] G. Gorfine. private communication.

[29] G. Gorfine and G. Taylor. Particle fluxes and damage to silicon in the ATLAS inner detector, 1994. ATLAS internal document INDET 030.

[30] H. Feick, E. Fretwurst, G. Lindström and M. Moll. Long term damage studies using silicon detectors fabricated from different starting materials and irradiated with neutrons, protons, and pions. Presented at 7th European Symposium on Semiconductor Detectors, Elmau, May 7-10, 1995, submitted to Nuclear Instruments and Methods, 1995.

[31] S.J. Bates, C. Furetta, M. Glaser, F. Lemeilleur, C. Soave, and E. Leon Florian. Damage induced by pions in silicon detectors. *Nuclear Physics B (Proc. Suppl.)*, 44:510, 1995.

[32] T. Angelescu and A. Vasilescu. Comparative radiation hardness results obtained from various neutron sources and the NIEL problem. Contr. to the Conference on large scale application and radiation hardness of semiconductor detectors, Florence, June 1995, to be published in Nuclear Instruments and Methods, 1995.

[33] V.A.J. van Lint, T.M. Flanagan, R.E. Leadon, J.A. Naber and V.C. Rogers. *Mechanisms of Radiation Effects in Electronic Materials*, volume 1. John Wiley & Sons, 1980.

[34] J.W. Corbett. Radiation damage in silicon and germanium. In *Radiation effects*, pages 3–10. Gordon and Breach, Science Publishers Ltd, 1970.

[35] G.P. Mueller, N.D. Wilsey and M. Rosen. The structure of displacement cascade in silicon. *IEEE Transactions on Nuclear Science*, NS-29(6):1493, 1982.

[36] R. Wunstorf. Systematische Untersuchungen zur Strahlenresistenz von Silizium-Detektoren für die Verwendung in Hochenergiephysik-Experimenten. PhD thesis, Universität Hamburg, see also DESY FH1K-92-01, October 1992.

[37] R. Böttger et al. Radiation damage studies of high resistivity silicon detectors at various neutron energies. *Nucl. Instr. & Meth. in Physics Research*, to be published, 1996.

[38] M.S. Lazo, D.M. Woodall and P.J. McDaniel. Silicon and silicon dioxide neutron damage functions. In *Proc. Fast Burst React. Workshop, 1986*, pages 85–103. Sandia National Laboratories, 1987. [Tech. Rep.] SAND, SAND87-0098 Vol.1.

[39] A. Van Ginneken. Non ionizing energy deposition in silicon for radiation damage studies. Technical Report FN-522, Fermi National Accelerator Laboratory, October 1989.

[40] ASTM Subcommittee E-10.07 on Radiation effects on Electronic Materials, Components, and Devices. Standard practice for characterizing neutron energy fluence spectra in terms of an equivalent monoenergetic neutron fluence for radiation-hardness testing of electronics. In *Annual Book of ASTM Standards,*

Vol 12.02, chapter ASTM E722-85, pages 324–329. ASTM Committee E-10 on Nuclear Technology and Application, May 1985.

[41] G.D. Watkins. *Radiation damage in semiconductors.* Dunod, Paris, 1965. edited by P. Baruch.

[42] B.G. Svensson and J.L.Lindström. Generation of divacancies in silicon by MeV electrons : dose rate dependence and influence of Sn and P. *J. Appl. Phys.*, 72(12):5616, December 1992.

[43] B.R. Gossick. Disordered regions in semiconductors bombarded by fast neutrons. *Journal of Applied Physics*, 30(6), 1959.

[44] L.S. Smirnov. *A Survey of Semiconductor Radiation Techniques.* Mir Publishers, Moscow, 1983.

[45] J.W. Corbett. *Electron Radiation Damage in Semiconductors and Metals.* Academic Press, 1966.

[46] G.D. Watkins, J.R. Troxell and A.P. Chatterjee. Vacancies and interstitials in silicon. In J.H. Albany, editor, *Defects and Radiation Effects in Semiconductors, Conf. Ser. No. 46*, pages 16–30. The Institut of Physics, 1979.

[47] L. Palmetshofer and J. Reisinger. Defect levels in H^+-,D^+-, and He^+-, bombarded silicon. *J. Appl. Phys.*, 72(6):2167, September 1992.

[48] G.D. Watkins and J.W. Corbett. Defects in irradiated silicon : electron paramagnetic resonance of the divacancy. *Physical Review*, 138:A543, 1965.

[49] A.O. Evwaraye and E. Sun. Electron-irradiation-induced divacancy in lightly doped silicon. *J. Appl. Phys.*, 47(9):3776, 1990.

[50] B.G. Svensson and M. Willander. Generation of divacancies in silicon irradiated by 2-MeV electrons : Depth and dose dependence. *J. Appl. Phys.*, 62(7):2758, October 1987.

[51] L.C. Kimerling. New developments in defect studies in semiconductors. *IEEE Transactions on Nuclear Science*, NS23(6):1497, 1976.

[52] G.D. Watkins and J.W. Corbett. Defects in irradiated silicon. I. Electron spin resonance of the Si-A-center. *Physical Review*, 121(4):1001, 1961.

[53] J.W. Corbett, J.C. Bourgoin, L.J. Cheng, J.C. Corelli, Y.H. Lee, P.M. Mooney, and C. Weigel. The status of defect studies in silicon. *Inst. Phys. Conf. Ser.*, NS-35(31):1, 1977.

[54] G.D. Watkins and J.W. Corbett. Defects in irradiated silicon : electron paramagnetic resonance and electron-nuclear double resonance of the Si-E-center. *Physical Review*, 134:A1359, 1964.

[55] L.C. Kimerling, H.M. DeAngelis and C.P. Carnes. Annealing of electron-irradiated n-type silicon. I. Donor concentration dependence. *Physical Review*, B3(2):427, 1971.

[56] M.T. Asom, J.L. Benton, R. Sauer and L.C. Kimerling. Interstitial defect reactions in silicon. *Appl. Phys. Lett.*, 51(4):256, 1987.

[57] L.W. Song and G.D. Watkins. EPR identification of the single-acceptor state of interstitial carbon in silicon. *Physical Review*, B42(9):5759, 1990.

[58] G.D. Watkins and K.L. Brower. EPR-observation of the isolated interstitial catrbon atom in silicon. *Phy. Rev. Lett.*, 36:1329, 1976.

[59] L.C. Kimerling, P. Blood, and W.M. Gibson. n.n. In J.H. Albany, editor, *Defects and Radiation effects in Semiconductors, IOP Conf. Proc. Ser. No. 46*, page 273. IOP, 1979.

[60] J.M. Trombetta and G.D. Watkins. Identification of an interstitial carbon-interstitial oxygen complex in silicon. *Appl. Phys. Lett.*, 51(14):1103, 1987.

[61] P.M. Mooney, L.J. Cheng, M. Süli, J.D. Gerson, and J.W. Corbett. Defect energy levels in boron-doped silicon irradiated with 1 MeV electrons. *Physical Review*, B15(8):3836, 1977.

[62] L.W. Song, B.W.Benson and G.D.Watkins. Identification of a bistable defect in silicon: The carbon interstitial-carbon substitutional pair. *Appl. Phys. Lett.*, 51(15):1155, 1987.

[63] A. Chantre and L.C. Kimerling. Configurationally multistable defect in silicon. *Appl. Phys. Lett.*, 48(15), 1986.

[64] X.D. Zhan and G.D.Watkins. Electron paramagnetic resonance of multistable interstitial carbon-substitutional-group-V-atom pairs in silicon. *Physical Review*, B47(11):6363, 1993.

[65] E. Guerer, B.W. Benson,G.D. Watkins. Configurational metastability of carbon-phosphorus pair defects in silicon. *Materials Science Forum*, 83-87:339, 1992.

[66] X.D. Zhan and G.D.Watkins. EPR Study of multistable C_i-P_s in silicon. *Material Science Forum*, 83 -87:345, 1992.

[67] M. Moll. Temperungsexperimente an strahlengeschädigten Silizium-Detektoren. Diploma thesis, Universität Hamburg, 1995.

[68] G.E. Jellison. Transient capacitance studies of an electron trap E_c-E_t=0.105eV in phosphorus doped silicon. *J. Appl. Phys.*, 53(8):5715, 1982.

[69] P.V. Kuchinskii, V.M. Lomako, and L.N. Shakhlevich. Configurationally bistable defects in silicon. *JETP Lett.*, 43(9):544, 1986.

[70] L.W. Song, B.W.Benson and G.D.Watkins. Identification of a bistable defect in silicon: The carbon interstitial-carbon substitutional pair. *Appl. Phys. Lett.*, 51(15):1155, 1987.

[71] L.T. Ho and A.K. Ramdas. Excitation spectra and piezospectroscopic effects of magnesium donors in silicon. *Physical Review*, B5(2):462, 1972.

[72] S. Froyen and A. Zunger. Meta-stable impurities in semiconductors : Si:Mg and Si:Be. *Physical Review*, 34(10):7451, 1986.

[73] G. Lindström, M. Benkert, E. Fretwurst, T. Schulz and R. Wunstorf. Radiation effects in Si-detectors and calorimeter considerations. In D.F. Anderson, M. Derrick, H.E. Fisk, A. Para and C.M. Sazama, editor, *Proceedings of the First International Conference on Calorimetry in High Energy Physics; Fermi Lab, Batavia/Illinois, Oct./Nov. 1990*, pages 467–476, Singapore, New Jersey, London, Hong Kong, 1991. World Scientific.

[74] Z. Li and H.W. Kraner. Studies of frequency dependent CV characteristics of neutron irradiated p^+-n silicon detectors. *IEEE Transactions on Nuclear Science*, 38(2):244, 1991.

[75] H. Feick. Temperaturabhängigkeit der Langzeitausheilung neutronengeschädigter Silizium-Detektoren. Diploma thesis, Universität Hamburg, 1993.

[76] F. Lemeilleur, M. Glaser, E.H.M. Heijne, P. Jarron, E. Occelli, and J. Rioux. Electrical properties and charge collection efficiency for neutron-irradiated p-type and n-type silicon detectors. Nucl. Physics B (proc. Suppl.) 32, 1993. 415.

[77] F. Anghinolfi et al. Some recent results of the silicon detector radiation damage study by the RD2 collaboration. *Nucl. Instr. & Meth. in Physics Research*, A360:455, 1995.

[78] S.J. Bates. The effects of proton and neutron irradiations on silicon detectors at LHC. PhD thesis, Cambridge University, 1993.

[79] F.J. Morin and J.P. Maita. Electrical properties of silicon containing arsenic and boron. *Physical Review*, 96, 1954.

[80] D.A. Neamen. *Semiconductors Physics and Devices. Basic principles.* Irvin, Homewood, IL, 1992.

[81] D. V. Lang. Deep Level Transient Spectroscopy : A new method to characterize traps in semiconductors. *J. Appl. Phys.*, 45:3023, 1974.

[82] M. Okuyama, H. Takakura, and Y. Hamakawa. Fourier-transformation analysis of deep level transient signals in semiconductors. *Solid State Electronics*, 26:689, 1983.

[83] P.D. Kirchner, W.J. Schaff, G.N. Maracas, L.F. Eastman, T.I. Chappel and C.M. Ransom. The analysis of exponential and nonexponential transients in deep-level transient spectroscopy. *J. Appl. Phys.*, 52:6462, 1981.

[84] K. Ikeda and H. Takaoka. Analysis of transient response by means of discrete Fourier transformation. *J. Appl. Phys.*, 54:6031, 1983.

[85] S. Weiss. Halbleiteruntersuchungen mit dem DLTFS - (Deep-Level Transient Fourier Spectroscopy -) verfahren. PhD thesis, Universität Kassel, January 1991.

[86] S. Weiss and R. Kassing. Deep level transient Fourier spectroscopy (DLTFS - A technique for the analysis of deep level properties. *Solid State Electronics*, 31(12):1733, 1988.

[87] M.G. Buehler. Impurity centers in pn-junctions determined from shifts in the thermally stimulated current and capacitance response with heating rate. *Solid State Electronics*, 15:69–79, 1972.

[88] J.C. Muller, R. Stuck, R. Berger and P. Siffert. Thermally stimulated current measurements on silicon junctions produced by implantation of low energy boron ions. *Solid State Electronics*, 17:1293–1297, 1974.

[89] M. Bruzzi. TSC data-analysis on heavily irradiated silicon detectors. *Nucl. Instr. & Meth. in Physics Research*, A352:618, 1995.

[90] U. Biggeri. Tecniche sperimentale di analisi dei difetti prodotti per irraggiamento neutronico in silico ad alta resistivita. Tesi di laurea, Universita Firenze, Februar 1992.

[91] Gruppe Nukleare Messtechnik. I. Institut für Experimentalphysik der Universität Hamburg, 22053 Hamburg, Germany.

[92] Ketek GmbH. 81241 München-Pasing, Germany.

[93] Forschungszentrum Rossendorf e.V. 01474 Rossendorf, Germany.

[94] Micron Semiconductor Ltd. Lancing, Sussex, BN15 8UN, England.

[95] Intertechnique. 67383 Lingolsheim CEDEX, France.

[96] Max Planck Institut für Physik und extraterrestrische Physik. Halbleiterlabor, 81245 München, Germany.

[97] Wacker-Chemitronic. 84489 Burghausen, Germany.

[98] H.J. Brede, G. Dietze, K. Kudo, U.J. Schrewe, F. Tancu and C. Wen. Neutron yields from thick Be targets bombarded with deuterons or protons. Nucl. Instr. & Meth. in Physics Research, A274, 1989. 332-344.

[99] R. Schmidt. Neutronendosimetrie in gemischten Neutronen - Gamma - Feldern eines medizinisch genutzten ^{3}H(d,n)^{4}He-Generator. PhD thesis, Universität Hamburg, October 1978.

[100] A. Bock. Charakterisierung tiefer Störstellen mit dem DLTS-Verfahren. Diploma thesis, Universität Kassel, 1988.

[101] Boonton Electronics Corporation. 72B capacitance meter. Instruction manual, Randolph, New Jersey, 1988.

[102] L. Cohausz. private communication.

[103] D. Schümann. Temperaturabhängigkeit von neutroneninduzierten Schädigungseffekten in Silizium-Detektoren. Diploma thesis, Universität Hamburg, 1994.

[104] CTI-Cryogenics. Multiple uses of model 22C/350C cryodyne refrigerator. Instruction manual, Waltham, 1991.

[105] AME. Beschreibung zum AME-Kryostaten CRYODYN 91. Instruction manual, Berlin, 1994.

[106] LakeShore Cryotronics Inc. The model DRC-91CA temperature controller. Instruction manual, Ohio, 1990.

[107] Z. Li, W. Chen and H.W. Kraner. Effects of fast neutron radiation on the electrical properties of silicon detectors. *Nucl. Instr. & Meth. in Physics Research*, A308:585, 1991.

[108] D. Pitzl et al. Type inversion in silicon detectors. *Nucl. Instr. & Meth. in Physics Research*, A311:98, 1992.

[109] R. Wunstorf, M. Benkert, N. Claussen, N. Croitoru, E. Fretwurst, G. Lindström and T. Schulz. Results on radiation hardness of silicon detectors up to neutron fluences of 10^{15} n/cm^2. *Nucl. Instr. & Meth. in Physics Research*, A315:149–155, 1992.

[110] B. Sigfridsson and J.L. Lindström. Electrical properties of electron irradiated n-type silicon. *J. Appl. Phys.*, 47(10):4611, 1976.

[111] T. Wada, K. Yasuda, S.Ikuta, M.Takeda, and H. Masuda. Complex defects introduced into Si by high-energy electron irradiation : Production rates of defects in -n-Si. *J. Appl. Phys.*, 48(6):2145, 1977.

[112] Z. Li, V. Eremin, N. Strokan, and E. Verbitskaya. Investigation of the type inversion phenomena : resistivity and carrier mobility in the space charge region and electrical neutral bulk in neutron irradiated silicon p^+-n junction detectors. *IEEE Transactions on Nuclear Science*, 40(4):367–375, 1993.

[113] P.F. Lugakov, T.A. Lukashevich and V.V. Shusha. Nature of the defect determining the fermi-level stabilization in irradiated silicon. *phys.stat.sol. (a)*, 101(6), 1982.

[114] R. Wunstorf, M. Benkert, E. Fretwurst, G. Lindström, T. Schulz, R. Darvas, and N. Croitoru. Radiation damage of silicon detectors by monoenergetic neutrons between 1 and 14 MeV and 1.8 MeV electrons. *Nuclear Physics B (Proc. Suppl.)*, 23A, pages 324-332, July 1991. 2nd Int. Conf. on Advanced Technology and Particle Physics, Como/Italy, June 1990.

[115] H.W. Kraner, E. Fretwurst, and Z. Li. The use of the signal current pulse shape to study the internal electric field profile and trapping effects in neutron damaged silicon detectors. *Nucl. Instr. & Meth. in Physics Research*, A326:350, 1993.

[116] C. Osius. Untersuchungen von Siliziumdetektoren verschiedener Herstellungstechnologien mit einer 2 MeV-Scanningprotonenmikrostrahlsonde. Diploma thesis, Universität Hamburg, 1995.

[117] V. Eremin, Z. Li, and I. Iljashenko. Trapping induced N_{eff} and electrical field transformation at different temperatures in neutron irradiated high resistivity detectors. *Nucl. Instr. & Meth. in Physics Research*, A360:458, 1995.

[118] E. Fretwurst et al. Radiation hardness of silicon detectors for future colliders. *Nucl. Instr. & Meth. in Physics Research*, A326:357, 1993.

[119] S. Sotthibandu. Radiation damage studies of silicon detectors. PhD thesis, Imperial College, London, 1994.

[120] K. Gill, G. Hall, S. Roe, S. Sotthibandhu, R. Wheadon, P. Giubellino and L. Ramello. Radiation damage by neutrons and photons to silicon detectors. *Nucl. Instr. & Meth. in Physics Research*, A322:177, 1992.

[121] H.J. Ziock, et al. Temperature dependence of the radiation induced change of depletion voltage in silicon pin detectors. *Nucl. Instr. & Meth. in Physics Research*, A342:96, 1994.

[122] G. Beck, M. Gibson, T.W. Pritchard, and D. Robinson. Temperature dependence of reverse annealing in bulk damaged silicon. *Nuclear Physics B (Proc. Suppl.)*, 44:524, 1995.

[123] M. Moll, H. Feick, E. Fretwurst, G. Lindström and T. Schulz. Observation of a bistable defect generated and activated by heat treatments in irradiated high resistivity silicon detectors. *Nuclear Physics B (Proc. Suppl.)*, 44:468, 1995.

[124] A. Chilingarov, H. Feick, E. Fretwurst, G. Lindström and T. Schulz. Radiation studies and operational projections for silicon in the ATLAS inner detector. *Nucl. Instr. & Meth. in Physics Research*, A360:357, 1995.

[125] P. Gaworzewski and K. Schmalz. On the electrical activity of oxygen in silicon. *phys. stat sol. (a)*, 55, 1979.

[126] W.W. Keller. Pressure dependence of oxygen-related defect levels in silicon. *J. Appl. Phys.*, 55(10):3471, 1984.

[127] B. Pajot, J. Kauppinen, R. Anttila. High resolution study of the group V impurities absorption in silicon. *Solid State Communications*, 31:759, 1979.

[128] E. Verbitskaya, V.K. Eremin, A.M. Ivanov and N.B. Strokan. Deep levels in high-resistivity ultrapure n-type silicon. *Soviet Physics Semiconductor*, 26(11):1101, 1992.

[129] K. Nagasawa and M Schulz. Fast transient capacitance measurements for implanted deep levels in silicon. *Applied Physics*, 8:35, 1975.

[130] H.F. Wolf. *Silicon Semiconductor Data.* International Series of Monographs on Semiconductors. Pergamon Press, Oxford, London, Edinburgh, New York, Toronto, Sydney, Paris, Braunschweig, 1969.

[131] Y. Tokuda and A.Usami. Comparison of neutron and 2 MeV electron damage in n-type silicon by deep level transient spectroscopy. *IEEE Transactions on Nuclear Science*, 28(3):3564, 1981.

[132] J. Vanhellemont et al. Generation and annealing behaviour of MeV proton and 252 Cf irradiation induced deep levels in silicon diodes. *IEEE Transactions on Nuclear Science*, 41(3):479, 1994.

[133] L. Tulach, H. Frank, B. Sopko and Z. Brasil. Radiation defects in fast neutron-, electron-, and γ-irradiated silicon. *phys.stat.sol. (a)*, 100:K13, 1987.

[134] S.D. Brotherton and P. Bradley. Defect production and lifetime control in electron and γ-irradiated silicon. *J. Appl. Phys.*, 53(8):5720, 1982.

[135] P. Chaudhari, S.V. Bhoraskar, S. Padgavkar and V.N. Bhoraskar. Comparison of defects produced by 14-MeV neutrons and 1-MeV electrons in n-type silicon. *J. Appl. Phys.*, 70, 1991.

[136] Z. Su, A. Husain, and J.W. Farmer. Determination of oxygen in silicon by ratio of A center to E center. *J. Appl. Phys.*, 67(4):1903, Feb. 1990.

[137] J. Matheson, M.S. Robbins, and S.J. Watts. The effect of radiation induced defects on the performance of high resistivity silicon diodes. Technical Report RD20/TN/36, RD20, Geneva, Jan. 1995.

[138] J. Matheson, M.S. Robbins, S.J. Watts, G. Hall, and B. MacEvoy. A microscopic explanation for type inversion and the annealing behaviour of radiation damaged silicon detectors radiation induced defects on the performance. Technical Report RD20/TN/43, RD20, Geneva, May. 1995.

[139] U. Biggeri, E. Borchi, M. Bruzzi, Z. Li, and S. Lazanu. Studies of deep levels in high resistivity silicon detectors irradiated by high fluence neutrons using a thermally stimulated current spectrometer. *IEEE Transactions on Nuclear Science*, 41(4), August 1994.

[140] Z. Li. private communication.

[141] B. Papendick. Temperaturabhängigkeit von neutroneninduzierten Schädigungseffekten in Siliziumdetektoren. Diploma thesis, Universität Hamburg, October 1992.

[142] F. Lemeilleur et al. Study of characteristics of silicon detectors irradiated with 24 GeV/c protons between -20°C and +20°C . *Nucl. Instr. & Meth. in Physics Research*, A360:438, 1995.

[143] H. Feick. N.N. PhD thesis in preparation, Universität Hamburg, 1996.

Acknowledgements

This work has been carried out at the *Universität Hamburg* in the *Gruppe Nukleare Meßtechnik* under the guidance of Prof. Dr. Gunnar Lindström and Dr. Eckhart Fretwurst, and I wish to thank both of them for continuous support and many helpful discussions and advice.

I am indebted to Uwe Pein for his untiring technical support, which has been indispensable for the success of this work. I must also mention and thank Harald Schatz, who died in 1993, and Sascha Epifantsev for the preparation of excellent test detectors.

For the many helpful discussions and advice concerning software, literature and other physical and non-physical items, I offer my thanks to Henning Feick and Michael Moll. Very special thanks and wishes go to Renate Wunstorf, who became a good friend of mine and my family. She never hesitated to help, especially when time was short and open copy-shops rare.

During the time I spent working on this thesis many diploma students became members of our group and later on *Diplom Physiker*. For the funny time and the good team-work I like to thank especially Carsten Dehn, Parwin Heydarpoor, Bernd Papendick, Carsten Osius and Philipp Schlichthärle.

I also wish to thank Martin Eberle, Wolfgang Hildesheimer, Enrico Panaro, Mattias Seidel and all the other 'pluggies' for being nice and helpful colleagues or even more to me.

A hearty 'thanks' also goes to everyone else in the group for making my time here such a memorable one.

This work would have been unthinkable without the support of the irradiation facilities. I am indebted to Dr. R. Böttger, Dr. H. Schölermann, and the crew at the PTB and to Dr. A. Hess, H. Thurmann, and M. Thom at the UKE, for making even unusual set-ups possible.

Furthermore I like to thank Dres. A. Bock, L. Cohauzs and S. Weiss for many helpful discussions concerning DLTS.

During the visits of several conferences and RD2-meetings I became acquainted with many physicists from foreign universities and institutes. I must mention Steven Bates from Cambridge (now at CERN), Francois Lemeilleur from CERN, Zheng Li from BNL, Andreas Rolf from Dortmund, and Ugo Biggeri from Firenze who became also a good friend. All of them and also those I did not mention I like to thank for making scientific and social life so exciting.

I am grateful to Susan and Steven Coverly who helped to avoid howlers like 'fluence of desire' and who skipped a lot of 'respectivelies' which were simply unnecessary.

I dedicate this thesis to Inken and Jobst Roderick for their encouragement over the years and months respectively. Their love and care helped me especially in the last few months to write and finish this thesis.

List of Publications

1. R. Wunstorf, M. Benkert, E. Fretwurst, G. Lindström, T. Schulz, N. Croitoru, R. Darvas, M. Mudrik, R. Böttger, and H. Schölermann : Radiation damage of silicon detectors by monoenergetic neutrons and electrons, *Nuclear Physics B (Proc. Suppl.), 23A, p. 324*, 1991.

2. E. Fretwurst, N. Claussen, N. Croitoru, G. Lindström, B. Papendick, U. Pein, H. Schatz, T. Schulz, and R. Wunstorf : Radiation hardness of silicon detectors for future colliders, *Nucl. Instr. & Meth. in Physics Research A 326, p. 357*, 1993.

3. F. Anghinolfi, R. Bardos, S.J. Bates, R. Bonino, A.G. Clark, N. Claussen, E. Fretwurst, M. Glaser, G. Gorfine, C. Gößling, E.H.M. Heijne, P. Jarron, R. Klingenberg, F. Lemeilleur, G. Lindström, G. Moorhead, D.J. Munday, E. Occelli, H. Pagel, B. Papendick, M.A. Parker, D. Pollmann, A. Poppleton, A. Rolf, P. Scampoli, T. Schulz, G. Taylor, S. Tovey, A.R. Weidberg, X. Wu and R. Wunstorf (CERN Detector R& D Collaboration RD-2) : neutron irradiation of silicon diodes at temperatures of +20°C and -20°C, *Nucl. Instr. & Meth. in Physics Research A 326, p. 365*, 1993.

4. E. Fretwurst, H. Feick, M. Glaser, C. Gößling, E.H.M. Heijne, A. Hess, F. Lemeilleur, G. Lindström, K.H. Mählmann, A. Rolf, T. Schulz, and C. Soave (CERN Detector R& D Collaboration RD-2) : Reverse annealing of the effective impurity concentration and long term operational scenario for silicon detectors in future collider experiments, *Nucl. Instr. & Meth. in Physics Research A 342, p. 119*, 1994.

5. S.J. Bates, D.J. Munday, M.A. Parker, F. Anghinolfi, A. Chiligarov, A. Ciasnohova, M. Glaser, E. Heijne, P. Jarron, F. Lemeilleur, J.C. Santiard, R. Bonino, A.G. Clark, H. Kambara C. Gössling, B. Lisowski, A. Rolf, S. Pilath, H. Feick, E. Fretwurst, G. Lindström, T. Schulz, R.A. Bardos, G.W. Gorfine, G.F. Moorhead, G.N. Taylor, and S.N. Tovey (CERN Detector R& D Collaboration RD-2) : Recent results of radiation damage studies in silicon, *Nucl. Instr. & Meth. in Physics Research A 344, p. 228*, 1994.

6. T. Schulz, H. Feick, E. Fretwurst, G. Lindström, M. Moll, and K.H. Mählmann : Long term reverse annealing in silicon detectors, *IEEE Transactions on Nuclear Science, Vol.41, p. 791*, 1994.

7. M. Moll, H. Feick, E. Fretwurst, G. Lindström, and T. Schulz : Observation of a bistable defect generated and activated by heat treatments in irradiated high resistivity silicon, Submitted to *Nuclear Physics B*, 1994.

8. E. Fretwurst, C. Dehn, H. Feick, P. Heydarpoor, G. Lindström, M. Moll, C. Schütze, and T. Schulz : Neutron induced defects in silicon detectors characterized by DLTS and TSC methods, submitted to *Nucl. Instr. & Meth. in Physics Research A* 1995.